

Published in final edited form as:

Int J Cancer. 2012 November 1; 131(9): 2143–2152. doi:10.1002/ijc.27471.

Efficacy of anti-insulin like growth factor I receptor (IGF-IR) monoclonal antibody cixutumumab in mesothelioma is highly correlated with IGF-IR sites/cell

Neetu Kalra¹, Jingli Zhang¹, Yunkai Yu², Mitchell Ho¹, Maria Merino³, Liang Cao², and Raffit Hassan¹

¹Laboratory of Molecular Biology, National Cancer Institute, National Institutes of Health, Bethesda, MD 20892

²Genetics Branch, National Cancer Institute, National Institutes of Health, Bethesda, MD 20892

³Laboratory of Pathology, Center for Cancer Research, National Cancer Institute, National Institutes of Health, Bethesda, MD 20892

Abstract

Insulin growth factor-I receptor (IGF-IR) is expressed in mesothelioma and therefore an attractive target for therapy. The anti-tumor activity of cixutumumab, a humanized monoclonal antibody to IGF-IR, in mesothelioma and relationship to IGF-IR expression was investigated using eight early passage tumor cells obtained from patients, nine established cell lines and an *in vivo* human mesothelioma tumor xenograft model. Although IGF-IR expression at the mRNA and protein level was present in all mesothelioma cells, using a quantitative ELISA immunoassay there was considerable variability of IGF-IR expression ranging from 1 to 14 ng/mg of lysate. Using flow cytometry the number of IGF-IR surface receptors varied from \approx 2,000 to 50,000 sites/cell. Cells expressing >10,000 sites/cell had greater than 10% growth inhibition when treated with cixutumumab (100 μ g/mL). Cixutumumab also induced antibody-dependent cell-mediated toxicity (ADCC) (>10% specific lysis) in cell lines, which had >20,000 IGF-IR sites/cell. Treatment with cixutumumab decreased phosphorylation of IGF-IR, Akt and Erk in cell lines, H226 and H28 having 24,000 and 51,000 IGF-IR sites/cell respectively but not in the cell line H2052 with 3,000 IGF-IR sites/cell. *In vivo*, cixutumumab treatment delayed growth of H226 mesothelioma tumor xenografts in mice and improved the overall survival of these mice compared to mice treated with saline ($p < 0.004$). Our results demonstrate that the anti-tumor efficacy of cixutumumab including inhibition of IGF-IR downstream signaling is highly correlated with IGF-IR sites/cell. A phase II clinical trial of cixutumumab is currently ongoing for treatment of patients with mesothelioma.

Keywords

Malignant mesothelioma; IGF-IR; Cixutumumab; ADCC; Pleural mesothelioma

Introduction

Malignant mesothelioma (MM) is an aggressive tumor associated with prior asbestos exposure that arises from the mesothelial cells lining the pleura, peritoneum and pericardium.¹ Although patients who present with limited tumor burden may benefit from

surgical resection, the majority of the patients at diagnosis have advanced disease and are not candidates for surgery.² Combination chemotherapy with pemetrexed and cisplatin has been shown to improve overall survival in patients with pleural mesothelioma but it results in a median overall survival of only 12.1 months.³ Thus, there is clearly a need to develop more effective treatments to improve the prognosis of these patients.

The insulin growth factor (IGF) signaling pathway consisting of the receptors I and II (IGF-IR and IGF-IIR), the ligands IGF-I and IGF-II, and IGF binding proteins (IGFBPs), has been implicated in the tumorigenesis of many different cancers. These studies have shown that signaling via the IGF-IR results in cell proliferation, invasion, and metastasis.^{4,5} Using normal mesothelial and established mesothelioma cell lines Lee *et al.* demonstrated that IGF-I functions as an autocrine growth stimulus for normal proliferating mesothelial cells and dysregulation of this loop may lead to their malignant transformation.⁶ Hoang *et al.* characterized the IGF signaling pathway in mesothelioma using primary tumor samples, as well as established cell lines.⁷ Activation of the insulin receptor substrates (IRS) 1 and 2 was shown in response to binding of IGF-I to IGF-IR leading to activation of the phosphatidylinositol 3-kinase (pI3K)/Akt pathway. Activation of IRS-1 increased cell growth while IRS-2 activation resulted in increased cell motility.

The utility of the IGF-IR as a potential therapeutic target for treatment of MM was demonstrated in an *in vivo* SV40-induced, immunocompetent hamster mesothelioma model that showed delay in tumorigenesis by using IGF-IR antisense transcripts.⁸ Small molecule tyrosine kinase inhibitors, such as NVP-AEW541 and AG1024, that inhibit the phosphorylation of IGF-IR have shown anti-proliferative activity against mesothelioma cell lines *in vitro*.^{9,10} These studies highlight the role of IGF-IR signaling as a therapeutic target in MM.

Another strategy to inhibit the signaling via IGF-IR is the use of monoclonal antibodies (mAbs) that block the interaction of IGF-IR to its ligands and in comparison to small molecule inhibitors have the potential advantage of inhibiting only IGF-IR and not insulin receptor (IR) signaling.⁵ Several anti-IGF-IR mAbs are in various stages of clinical development for treatment of different tumors.^{11,12} One of these mAbs is cixutumumab (IMC-A12), a fully human IgG1 mAb that has been shown to possess anti-tumor activity in a wide variety of *in vitro* and *in vivo* tumor models including breast, colon, pancreatic and prostate cancer.¹³ Cixutumumab binds IGF-IR leading to surface receptor internalization and degradation.¹⁴ The goals of our study were to characterize in detail IGF-IR expression in mesothelioma using tumor cells obtained from patients as well as established cell lines, to evaluate the anti-tumor efficacy of cixutumumab and to identify factors that influence its activity.

Materials and Methods

Reagents and cell lines

Cixutumumab, a fully humanized mAb to IGF-IR, was provided by ImClone Systems Inc. (New York, NY). The human mesothelioma cell lines MSTO211H, H28, H226, H2452, H2052 were obtained from American Type Culture Collection (Manassas, VA). The mesothelioma cell line M60 was a gift from Dr. Steven Albelda (University of Pennsylvania) and the normal mesothelial cell line LP-9 was purchased from the cell culture core facility at Harvard University (Boston, MA). Cell culture related reagents except fetal bovine serum (FBS) were purchased from Invitrogen/Life Technologies, Inc., (Rockville, MD). FBS was purchased from Lonza Walkersville, Inc. (Walkersville, MD). All cells except LP-9 were cultured in RPMI-1640 supplemented with 10% FBS, 2 mM glutamine and 10 µg/ml penicillin/streptomycin. LP-9 was cultured in M199 containing 15% FBS, 10

ng/mL EGF and 0.4 µg/mL hydrocortisone. All cells were cultured at 37°C in 5% CO₂ humidified air.

Patient specimens

Ascites or pleural effusion samples were obtained from 8 patients with MM (7 peritoneal and 1 pleural) undergoing treatment at the Clinical Research Center, National Institute of Health (NIH). These samples were obtained with approved protocols from the National Cancer Institute (NCI) institutional review board. Tumor cells were isolated from neoplastic effusions by centrifugation and resuspended in RPMI-1640 medium with 10% FBS. The cells were plated in tissue culture dishes and remained in culture until they became confluent, before the first passage. All early passage cells used in the experiments described below were within 3 passages.

RNA isolation and real time PCR assay

RNA extraction from each cell line was done as described previously.⁷ Briefly, for total RNA (2 µg) extraction, the Trizol method was used with a silica gel-based membrane spin column (Qiagen, Valencia, CA). cDNA was synthesized using a Superscript III kit (Invitrogen, Rockville, MD) and quantitative PCR (qPCR) reactions were performed using QuantiTect SYBR Green PCR kit (Qiagen) on a Bio-Rad iCycler. The C_t values obtained were normalized to GAPDH.

Electrochemiluminescence (ECL) assay to quantify IGF-IR level

The ECL assay for quantitation of total IGF-IR level in each cell line was done as described earlier.¹⁵ Briefly, 36 µg/mL of anti-IGF-IR antibody from R&D Systems (Minneapolis, MN) was coated on 96 well assay plates in coating buffer (0.015% Triton X-100 in phosphate buffered saline [PBS]) overnight at 4°C. Next day, 1 mg/ml of cell lysates were added to each well after blocking with 3% bovine serum albumin (BSA). Lysates were incubated with antibody for 2 hr at room temperature with constant shaking. Cells were washed and incubated with 400ng/mL of biotin-anti-IGF-IR detection antibody for 1 hr. For signal detection, 1 µg/mL of SULFO-TAG streptavidin (MSD, Gaithersburg, MD) was added and incubated for 1 hr, followed by detection with MSD read buffer.

Western blot analysis of IGF-IR protein expression in mesothelioma cell lines

Monolayers of confluent cells were washed twice in PBS, and then lysed in 1X Cell Lysis Buffer supplemented with 1 mM phenylmethylsulfonyl fluoride (PMSF) (Cell Signaling Technology, Beverly, MA). Fifty µg of total protein was subjected to SDS-polyacrylamide gel electrophoresis (Invitrogen) for each cell line followed by immunoblotting with anti-IGF-IR mouse mAb (1:1000 in 5% blocking reagent in Tris-buffered saline/Tween-20) from Cell Signaling Technology overnight at 4°C. The following day blots were incubated with goat anti-mouse IgG conjugated with horseradish peroxidase (HRP) (Santa Cruz Biotechnology, Santa Cruz, CA; 1:1000 dilution) for 1 hr at 25°C. Signals were visualized with the enhanced chemiluminescence reagent (Amersham Pharmacia Biotech, Piscataway, NJ) on X-ray film (Eastman Kodak, Rochester, NY). To evaluate the effect of cixutumumab on IGF-IR downstream signaling pathways cell lysates of H28, H226 and H2052 cell lines were prepared using the same protocol as described above. Cells were incubated with 100 µg/ml of cixutumumab in serum free medium overnight. The next day cells were treated with or without IGF-I (50 ng/mL) for 15 min and harvested for western blot using IGF-IR, p-IGF-IR (Tyr 1316), Akt, p-Akt (Ser 473), Erk 1/2 and p-Erk1/2 (Thr 202/Tyr 204), antibodies (Cell Signaling Technology).

Immunohistochemistry (IHC) for IGF-IR expression on tumor cells obtained from patients

Formalin fixed paraffin embedded cell blocks were prepared using the thrombin clot method and five micron sections were mounted on charged microscopic slides. IHC for IGF-IR expression was done using the anti-IGF-IR- β polyclonal antibody (Cell Signaling Technology). These IHC slides were evaluated by a pathologist (M.M.) experienced in diagnosis of mesothelioma and IHC. Each slide was scored for the percent of tumor cells that were positive for IGF-IR expression, as well as the intensity of staining.

Evaluation of cixutumumab binding to mesothelioma cells using flow cytometry

Cells (0.5×10^6) were harvested and washed twice with cold PBS. Nonspecific binding to Fc receptors was blocked by treatment with anti-Fc antibody (Sigma St. Louis, MO) for 15 min at room temperature. Cells were resuspended in 2% BSA/PBS, and incubated with cixutumumab or an isotype control antibody at the final concentration of $10 \mu\text{g}/1 \times 10^6$ cells at 4°C for 1 hr. After washing, cells were incubated with a goat anti-human IgG phycoerythrin-conjugated secondary antibody (Pharmingen, BD Biosciences, San Jose, CA) for an additional 1 hr at 4°C and were analyzed for cixutumumab surface binding using a flow cytometer (FACS Calibur, BD Biosciences). Data was analyzed using FlowJo (Tree Star, Inc., Ashland, OR).

Cell surface IGF-IR quantitation

QuantiBRITE PE beads (BD Biosciences) having each of the four bead populations with a calibrated mean number of bound phycoerythrin (PE) molecules/bead was used to establish a fluorescence standard. Cells (0.5×10^6) were harvested and washed with 2% BSA/PBS twice. Cells were stained with anti-IGF-IR mAb ($10 \mu\text{g}/1 \times 10^6$ cells at 4°C for 1 hr) (BD Biosciences) conjugated with PE at a 1:1 ratio. Cells were acquired using CellQuest Pro software on FACS Calibur and analyzed for FL-2 H geometric mean using FlowJo software. The number of bound PE-conjugated antibodies/cell in the sample was extrapolated using PE beads as a standard. Quantitation of receptor site per cell was done using equation, $y = mx + c$, where y equals Log_{10} uorescence and x equals Log_{10} PE molecules per bead.

Effect of cixutumumab on mesothelioma cell viability

Cell viability was determined using a ATPlite 1-step luminescence detection assay (Perkin-Elmer, Fremont, CA). Cells (5,000–10,000 per well) in exponential growth were seeded on a 96-well plate and incubated in 10% RPMI complete growth medium overnight. After 24 hr, complete medium was removed from the wells and replaced with medium with 2% FBS containing either cixutumumab (experimental) or human IgG (control) in a range between 0 and $100 \mu\text{g}/\text{mL}$ with three replicates per dose. Cells were allowed to grow in culture for 72 hr and then $50 \mu\text{l}$ of ATP Lite solution was added to each well. ATP Lite assay was performed based on the manufacturer's protocol and results recorded using a Victor 3 plate reader (Perkin-Elmer).

siRNA knockdown of IGF-IR in the mesothelioma H28 cell line

Trilencer-27 human siRNA against IGF-IR and scrambled control were purchased from Origene (Rockville, MD) and RNA interference assay was done according to the manufacturer's protocol. Briefly, H28 cells were seeded in 6-well culture plates at 30% confluence in RPMI medium supplemented with 10% fetal bovine serum. The next day, cells were transfected with either IGF-IR or scrambled control siRNA for 48 hr at a final concentration of $100 \text{nmol}/\text{L}$ by using Turbofectin transfection reagent (Origene). IGF-IR expression in these cells was then determined by Western blot analysis.

Determination of cixutumumab mediated ADCC

Peripheral blood mononuclear cells (PBMC) (Department of Transfusion Medicine, NIH Clinical Center) were isolated from healthy donors with Ficoll-Paque Plus (GE Healthcare, Piscataway, NJ). Target cells were incubated with 100 µg/ml of cixutumumab or IgG control antibody at 4°C for 60 min then added to effector cells at 10,000 cells per well in triplicates. The ratio of effector to target cells was 100:1. The plate was incubated at 37°C for 20 hr. Supernatant (100 µL) was transferred to an all-white plate, and 100 µL of CytoTox-ONE reagent (Roche, Indianapolis, IN), was added to each well. The lactate dehydrogenase released from lysed cells converted CytoTox substrate to fluorescent resazurin, which was measured in fluorometer (Ex 560 nm/Em 590 nm). Measurement of target cells alone treated with 2% Triton X100 was used as high control. The percentage of specific lysis was calculated as: (experimental treatment – effector cell control)/(high control-target cell control) × 100%.

In vivo human mesothelioma xenograft model

H226 cells stably transfected with GFP-luciferase fusion proteins (LMB-H226-GL) were used to establish mesothelioma xenografts in 4–6 week-old female athymic nude mice (NCI-Frederick Animal Production Area, Frederick, MD) as described previously.¹⁶ Five million H226 cells were inoculated i.p. into athymic nude mice. The tumor distribution was followed by serial whole-body non-invasive imaging of visible light emitted by luciferase expressing mesothelioma cells upon injection of mice with luciferin. Three days after injection of tumor cells, mice were divided into two groups (n = 9 mice in each group) with statistically equivalent tumor burden. Mice received either cixutumumab (50 mg/kg) or saline i.p. twice a week for the next 60 days. Body weight of each mouse was measured once a week throughout the study and after 60 days of treatment mice were screened for overall survival. Mice were given i.p. injections of luciferin every week, and bioluminescence imaging with a charge coupled device camera (IVIS, Xenogen, Alameda, CA) was initiated 5 min after injection. Data was quantified by Living Image R 3.1 software and expressed as photon emission (photons/s/cm²/steradian).

Statistical analysis

The data is presented as the mean ± SD. A two tailed student's t-test was used for statistical comparison and defined as statistically significant with P<0.05. Statistical analyses were performed using Prism (GraphPad).

Results

IGF-IR expression in established and early passage mesothelioma cells

The amount of IGF-IR in mesothelioma cell lysates was quantified using ECL assay.¹⁵ We used the breast cancer cell line MCF-7 as a positive control and the normal mesothelial cell line LP-9 as a negative control. The level of IGF-IR as determined by the ECL assay was 1.5 and 15 ng/mg of lysate in LP-9 and MCF-7 cells respectively. Most of the mesothelioma cell lines, except H2052, expressed higher amount of IGF-IR than LP-9 that ranged from 1–14ng/mg of lysate (Fig. 1A). The results on IGF-IR quantification by ECL assay were further confirmed by qPCR and western blot analysis with a different antibody against IGF-IR (Fig. 1B, 1C).

We also evaluated IGF-IR expression by IHC using cell blocks made from early passage mesothelioma cells grown in short-term culture. As shown in Figure 1D, all the cells had diffuse IGF-IR expression, both membranous and cytoplasmic, with the intensity of staining varying from 2+ to 3+. These results further confirmed the presence of IGF-IR in all early passage mesothelioma cells.

Cixutumumab binding to mesothelioma cell lines corresponds to IGF-IR sites per cell

The binding of cixutumumab to established and early passage mesothelioma cells was evaluated by flow cytometry. Our results showed that cixutumumab specifically bound to the mesothelioma cells but there was variability in its binding to the different cell lines (Fig. 2A, 2B). We next used highly specific QuantiBRITE-PE beads for cell surface IGF-IR quantification. Samples were stained with anti-IGF-IR antibody that was conjugated with PE at a 1:1 ratio so that the PE molecules bound/cell is equivalent to the number of antibodies bound to the cell. This, in turn, approximates the number of cell surface IGF-IR. We found differential relative surface expression in the range of 2,000–52,000 sites/cell among mesothelioma cell lines (Fig. 2C). Among the established mesothelioma cell lines H28 had the highest number (51,613) and H2052 the least number (3,813) of IGF-IR sites/cell. Among the early passage mesothelioma cells, the IGF-IR sites/cell ranged from 2,842 to 23,584. Our results demonstrate that the binding of cixutumumab to mesothelioma cells is dependent on cell surface IGF-IR expression.

Inhibition of mesothelioma cell viability correlates with the amount of IGF-IR surface receptor expression

Next, we examined how the differential expression of IGF-IR would affect the sensitivity of mesothelioma cell lines to cixutumumab. Among established cell lines, H28 expressing 51,613 IGF-IR sites/cell was the most sensitive cell line with 40% growth inhibition at the highest dose of cixutumumab (Fig. 3A) but it had no effect on the viability of H2052 cells that have 3,813 IGF-IR sites/cell. Pearson correlation analysis revealed a significant correlation between growth-inhibitory effects of cixutumumab and the surface levels of IGF-IR in the established MM cell lines (Fig. 3Aa). In early passage cells, NCI-M-13 was the most sensitive cell line with 29% cell growth inhibition followed by NCI-M-03 cell line with 20% inhibition (Fig. 3B). However, NCI-M-02, NCI-M-05 and NCI-M-07, which had minimal cell surface IGF-IR expression, showed minimal growth inhibition when treated with cixutumumab. Significant correlation was also obtained between surface IGF-IR expression and inhibition of cell growth in early passage cells (Fig. 3Bb).

To further characterize the effect of IGF-IR expression on sensitivity to cixutumumab, we did knockdown of IGF-IR in the H28 mesothelioma cell line. Depletion of IGF-IR was confirmed by Western blot analysis (Fig. 3Cc). Starting at 48 hr after knockdown, we treated these cells for another 72 hr with 10 or 100 $\mu\text{g}/\text{mL}$ of cixutumumab and cell viability was assessed using the ATP Lite assay. Cells transfected with IGF-IR siRNA were significantly more resistant to cixutumumab treatment ($p < 0.02$, Fig. 3C) in comparison to the cells treated with scrambled control siRNA.

Cixutumumab inhibits the IGF-IR downstream signaling in mesothelioma cell lines

We also looked for the effect of cixutumumab on downstream pathways of IGF-IR signaling by western blot analysis. Cixutumumab treatment down-regulated the phosphorylated levels of IGF-IR and Akt induced by IGF-I in H28 and H226 cell lines with high total expression of IGF-IR (Fig. 4). However, no effect could be seen on the phosphorylation of IGF-IR and Akt in H2052 cells expressing the least amount of IGF-IR among established MM cell lines. There was a moderate decrease in the phosphorylated levels of Erk in H226 and H28 cells. However, cixutumumab treatment had no effect on the phosphorylated levels of Erk in H2052 cells. The down-regulation of phosphorylated Akt was much more apparent than phosphorylated Erk (Fig. 4). Our results show that cixutumumab can inhibit signaling by blocking activation of Akt and up to some extent the activation of Erk pathway in MM cell lines.

Cixutumumab induces antibody mediated cell cytotoxicity in mesothelioma cells

The ability of cixutumumab to elicit ADCC was evaluated against several mesothelioma cell lines with varying degrees of IGF-IR expression by flow cytometry. As shown in Figure 5A treatment with cixutumumab in presence of effector cells induced >30% specific lysis in H28 cells, whereas control IgG in presence of PBMC or cixutumumab alone resulted in no specific cell lysis. H2052 cells, which have about 3,000 IGF-IR sites/cell, showed no specific lysis when treated with cixutumumab in presence of effector cells (Fig. 5B). The extent of ADCC induced by cixutumumab was dependent on the number of IGF-IR sites/cell with >10% specific lysis in cell lines with more than 20,000 IGF-IR sites/cell (Fig. 5C).

Cixutumumab delays tumor growth and improves survival in mesothelioma xenograft model

To assess the activity of cixutumumab on mesothelioma tumor growth *in vivo*, H226 cell (stably transfected with luciferase gene) tumor xenograft model was established in athymic nude mice. As shown in Figure 6A, treatment with cixutumumab twice a week for 60 days had significant growth inhibition. As early as day 14 of treatment with cixutumumab, the anti-tumorigenic effect was apparent in terms of decrease in total luminescence count in the cixutumumab treated group of mice in comparison to the saline treated control group (Fig. 6A). Figure 6B shows bioluminescence imaging in the mice treated with saline or cixutumumab on days 24 and 60 of treatment. The effect remained consistent throughout the study period. At the end of the treatment schedule, the animals were observed for overall survival. All mice were sacrificed following institutional ethical guidelines, either due to tumor progression or weight loss greater than 15% body weight. The mice treated with cixutumumab showed enhanced survival in comparison to the saline treated control group, 90 versus 81 days respectively ($p < 0.004$, Fig. 6C).

Discussion

In the present study we characterized IGF-IR expression in mesothelioma and its correlation with the anti-tumor activity of cixutumumab, a fully human mAb to IGF-IR. Since receptor expression can influence the activity of mAbs targeting it, we evaluated IGF-IR expression in mesothelioma using a variety of different methods. Using early passage tumor cells as well as established mesothelioma cell lines, we showed a wide variability in IGF-IR levels in these cells ranging from 1–14 ng/ml of the cell lysate. Using IHC we observed diffuse IGF-IR expression in all early passage mesothelioma cells. However, there was a significant variation in IGF-IR expression among cell lines when we quantified the number of surface IGF-IR sites/cell by flow cytometry. In established mesothelioma cell lines, IGF-IR sites/cell ranged from about 3,000–50,000 and in early passage mesothelioma cell lines, IGF-IR sites/cell ranged from about 2,000–23,000. The IGF-IR sites/cell correlated with IGF-IR mRNA and protein expression. However, IHC was not helpful to distinguish between cells with high and low IGF-IR levels since all the cell lines showed diffuse strong IGF-IR staining.

Our results also show that the anti-proliferative activity of cixutumumab against early passage and established mesothelioma cell lines correlated with the number of IGF-IR sites/cell. There was no growth inhibition by cixutumumab in cell lines with <10,000 IGF-IR sites/cell while cell lines that had greater than 10,000 IGF-IR sites/cell showed decreased viability in response to cixutumumab that correlated with IGF-IR sites/cell. Our results are in agreement with a prior report that showed the IGF-IR level in rhabdomyosarcoma cells affected the anti-proliferative activity of an anti-IGF-IR mAb.¹⁵ Similarly, in non-small cell lung cancer cell lines the cell growth inhibition by the anti-IGF-IR mAb R1507 was dependent on the total IGF-IR protein expression.¹⁷ However, both of these studies did not

directly evaluate the number of IGF-IR sites/cell. Rubini *et al.* have previously shown that IGF-IR numbers plays a role in IGF-I mediated mitogenesis and transformation of mouse embryo fibroblasts.¹⁸ Cells which had <15,000 IGF-IR sites/cell did not grow in serum free medium supplemented with IGF-I even in the presence of other growth factors, while cells with greater than 15,000 IGF-IR sites/cell were able to grow in serum free medium when supplemented only with IGF-I. Our results demonstrate that in mesothelioma cells IGF-IR number is an important factor to determine the efficacy of anti-IGF-IR mAb.

We also showed that cixutumumab decreased the phosphorylation of IGF-IR, Akt and Erk that was dependent on IGF-IR expression. In the cell lines H226 and H28 with high IGF-IR expression treatment with cixutumumab decreased phosphorylated IGF-IR, Akt and Erk but not in the cell line H2052 which had minimal IGF-IR expression.

In addition, to cixutumumab inhibiting the viability of mesothelioma cells by direct inhibition of the IGF-IR signal transduction pathway we show that it can also kill mesothelioma cells via ADCC. The ability of cixutumumab to induce cell death via ADCC was also dependent on IGF-IR expression. In cells lines with greater than 20,000 IGF-IR sites/cell treatment with cixutumumab resulted in greater than 10% specific lysis while as no effect was seen in the cell lines with minimal IGF-IR expression. The influence of cell surface receptor expression on the induction of ADCC has also been noted for other mAbs. Kimura *et al.* showed that the anti-epidermal growth factor receptor (EGFR) mAb cetuximab induced ADCC in various tumor cell lines which correlated with the surface levels of EGFR.¹⁹ The ability of cixutumumab to kill tumor cells via induction of ADCC has not been previously reported.

In addition to the *in vitro* activity of cixutumumab against mesothelioma cell lines, we also show that treatment with cixutumumab inhibits tumor growth of the human mesothelioma tumor xenograft H226 in nude mice. This cell line highly expresses IGF-IR and is sensitive to growth inhibition and induction of ADCC by cixutumumab.

The results of IGF-IR targeted mAbs have thus far shown mixed results in the clinic. Although a phase II clinical trial of the anti-IGF-IR mAb figitumumab in combination with chemotherapy showed significant anti-tumor activity in front line therapy of lung cancer, a subsequent phase III clinical trial was halted due to lack of efficacy.²⁰⁻²² Similarly, a randomized phase II study of cixutumumab in metastatic colorectal cancer showed no activity.²³ On the other hand, clinical trials of several anti-IGF-IR mAbs show encouraging activity in many different types of sarcomas.^{24,25} From the ongoing clinical trials of IGF-IR targeted therapies it is clear that better patient selection will be important to evaluate these agents. One of these variables includes tumor IGF-IR expression. Our results suggest that at least in mesothelioma, evaluation of tumor IGF-IR expression by IHC is not particularly useful since it may not be able to discriminate between high and low expression. Flow cytometry is a more sensitive method to quantitate IGF-IR expression and may be helpful in patients who have malignant pleural effusion or ascites. The findings from this study, in particular the correlation between IGF-IR expression and anti-tumor activity, could have implications for ongoing clinical trials of antibodies targeting IGF-IR. A phase II clinical trial of cixutumumab as a single agent is currently ongoing in patients with mesothelioma who have failed standard therapy.

Acknowledgments

The cixutumumab was generously provided by Imclone Systems, Inc. and NCI, NIH. This research was supported by the Intramural Research Program of the NIH, National Cancer Institute, Center for Cancer Research.

Abbreviations

ADCC	antibody-dependent cell-mediated cytotoxicity
BSA	bovine serum albumin
ECL	electrochemiluminescence
EGFR	epidermal growth factor receptor
FBS	fetal bovine serum
HRP	horseradish peroxidase
IGF	insulin growth factor
IGFBP	IGF binding protein
IGF-IR and IIR	IGF receptors I and II
IHC	immunohistochemistry
IR	insulin receptor
IRS	IR substrates
MM	malignant mesothelioma
mAbs	monoclonal antibodies
NCI	National Cancer Institute
NIH	National Institutes of Health
PBMC	peripheral blood mononuclear cells
PBS	phosphate buffered saline
PE	phycoerythrin
p13K	phosphatidylinositol 3-kinase
PMSF	phenylmethylsulfonylfluoride
qPCR	quantitative PCR

References

1. Robinson BW, Lake RA. Advances in malignant mesothelioma. *N Engl J Med.* 2005; 353:1591–603. [PubMed: 16221782]
2. Kaufman AJ, Flores RM. Surgical treatment of malignant pleural mesothelioma. *Curr Treat Options Oncol.* 2011; 12:201–16. [PubMed: 21465419]
3. Vogelzang N, Rusthoven JJ, Symanowski J, Denham C, Kaukel E, Ruffie P, Gatzemeier U, Boyer M, Emri S, Manegold C, Niyikiza C, Paoletti P. Phase III study of pemetrexed in combination with cisplatin versus cisplatin alone in patients with malignant pleural mesothelioma. *J Clin Oncol.* 2003; 21:2636–44. [PubMed: 12860938]
4. Pollak M. Insulin and insulin-like growth factor signalling in neoplasia. *Nat Rev Cancer.* 2008; 8:915–28.
5. Zha J, Lackner MR. Targeting the insulin-like growth factor receptor-1R pathway for cancer therapy. *Clin Cancer Res.* 2010; 16:2512–7. [PubMed: 20388853]
6. Lee TC, Zhang Y, Aston C, Hintz R, Jagirdar J, Perle MA, Burt M, Rom WN. Normal human mesothelial cells and mesothelioma cell lines express insulin-like growth factor I and associated molecules. *Cancer Res.* 1993; 53:2858–64. [PubMed: 7684950]

7. Hoang CD, Zhang X, Scott PD, Guillaume TJ, Maddaus MA, Yee D, Kratzke RA. Selective activation of insulin receptor substrate-1 and -2 in pleural mesothelioma cells: association with distinct malignant phenotypes. *Cancer Res.* 2004; 64:7479–85. [PubMed: 15492273]
8. Pass HI, Mew DJ, Carbone M, Matthews WA, Donington JS, Baserga R, Walker CL, Resnicoff M, Steinberg SM. Inhibition of hamster mesothelioma tumorigenesis by an antisense expression plasmid to the insulin-like growth factor-1 receptor. *Cancer Res.* 1996; 56:4044–8. [PubMed: 8752177]
9. Whitson BA, Jacobson BA, Frizelle S, Patel MR, Yee D, Maddaus MA, Kratzke RA. Effects of insulin-like growth factor-1 receptor inhibition in mesothelioma. Thoracic Surgery Directors Association Resident Research Award. *Ann Thorac Surg.* 2006; 82:996–1001. [PubMed: 16928523]
10. Kai K, D'Costa S, Sills RC, Kim Y. Inhibition of the insulin-like growth factor 1 receptor pathway enhances the antitumor effect of cisplatin in human malignant mesothelioma cell lines. *Cancer Lett.* 2009; 278:49–55. [PubMed: 19178995]
11. Rodon J, DeSantos V, Ferry RJ Jr, Kurzrock R. Early drug development of inhibitors of the insulin-like growth factor-I receptor pathway: lessons from the first clinical trials. *Mol Cancer Ther.* 2008; 7:2575–88. [PubMed: 18790742]
12. Gualberto A, Pollak M. Emerging role of insulin-like growth factor receptor inhibitors in oncology: early clinical trial results and future directions. *Oncogene.* 2009; 28:3009–21. [PubMed: 19581933]
13. Rowinsky EK, Youssoufian H, Tonra JR, Solomon P, Burtrum D, Ludwig DL. IMC-A12, a human IgG1 monoclonal antibody to the insulin-like growth factor I receptor. *Clin Cancer Res.* 2007; 13(18 Suppl):5549s–55s. [PubMed: 17875788]
14. Burtrum D, Zhu Z, Lu D, Anderson DM, Prewett M, Pereira DS, Bassi R, Abdullah R, Hooper AT, Koo H, Jimenez X, Johnson D, et al. A fully human monoclonal antibody to the insulin-like growth factor I receptor blocks ligand-dependent signaling and inhibits human tumor growth in vivo. *Cancer Res.* 2003; 63:8912–21. [PubMed: 14695208]
15. Cao L, Yu Y, Darko I, Currier D, Mayeenuddin LH, Wan X. Addiction to elevated insulin-like growth factor I receptor and initial modulation of the AKT pathway define the responsiveness of rhabdomyosarcoma to the targeting antibody. *Cancer Res.* 2008; 68:8039–48. [PubMed: 18829562]
16. Feng M, Zhang J, Anver M, Hassan R, Ho M. In vivo imaging of human malignant mesothelioma grown orthotopically in the peritoneal cavity of nude mice. *J Cancer.* 2011; 2:123–31. [PubMed: 21479131]
17. Gong Y, Yao E, Shen R, Goel A, Arcila M, Teruya-Feldstein J, Zakowski MF, Frankel S, Peifer M, Thomas RK, Ladanyi M, Pao W. High expression levels of total IGF-1R and sensitivity of NSCLC cells in vitro to an anti-IGF-1R antibody (R1507). *PLoS One.* 2009; 4(10):e7273. [PubMed: 19806209]
18. Rubini M, Hongo A, D'Ambrosio C, Baserga R. The IGF-I receptor in mitogenesis and transformation of mouse embryo cells: role of receptor number. *Exp Cell Res.* 1997; 230:284–92. [PubMed: 9024787]
19. Kimura H, Sakai K, Arao T, Shimoyama T, Tamura T, Nishio K. Antibody-dependent cellular cytotoxicity of cetuximab against tumor cells with wild-type or mutant epidermal growth factor receptor. *Cancer Sci.* 2007; 98:1275–80. [PubMed: 17498200]
20. Karp DD, Paz-Ares LG, Novello S, Haluska P, Garland L, Cardenal F, Blakely LJ, Eisenberg PD, Langer CJ, Blumenschein G Jr, Johnson FM, Green S, et al. Phase II study of the anti-insulin-like growth factor type 1 receptor antibody CP-751,871 in combination with paclitaxel and carboplatin in previously untreated, locally advanced, or metastatic non-small-cell lung cancer. *J Clin Oncol.* 2009; 27:2516–22. [PubMed: 19380445]
21. Gualberto A, Hixon ML, Karp DD, Li D, Green S, Dolled-Filhart M, Paz-Ares LG, Novello S, Blakely J, Langer CJ, Pollak MN. Pre-treatment levels of circulating free IGF-1 identify NSCLC patients who derive clinical benefit from figitumumab. *Br J Cancer.* 2011; 104:68–74. [PubMed: 21102589]
22. Basu B, Olmos D, de Bono JS. Targeting IGF-1R: throwing out the baby with the bathwater? *Br J Cancer.* 2011; 104:1–3. [PubMed: 21206496]

23. Reidy DL, Vakiani E, Fakih MG, Saif MW, Hecht JR, Goodman-Davis N, Hollywood E, Shia J, Schwartz J, Chandrawansa K, Dontabhaktuni A, Youssoufian H, et al. Randomized, phase II study of the insulin-like growth factor-1 receptor inhibitor IMC-A12, with or without cetuximab, in patients with cetuximab- or panitumumab-refractory metastatic colorectal cancer. *J Clin Oncol*. 2010; 28:4240–6. [PubMed: 20713879]
24. Olmos D, Postel-Vinay S, Molife LR, Okuno SH, Schuetz SM, Paccagnella ML, Batzel GN, Yin D, Pritchard-Jones K, Judson I, Worden FP, Gualberto A, et al. Safety, pharmacokinetics, and preliminary activity of the anti-IGF-1R antibody figitumumab (CP-751,871) in patients with sarcoma and Ewing's sarcoma: a phase 1 expansion color study. *Lancet Oncol*. 2010; 11:129–35. [PubMed: 20036194]
25. Olmos D, Tan DS, Jones R, Judson IR. Biological rationale and current clinical experience with anti-insulin-like growth factor 1 receptor monoclonal antibodies in treating sarcoma: twenty years from the bench to the bedside. *Cancer J*. 2010; 16:183–94. [PubMed: 20526094]

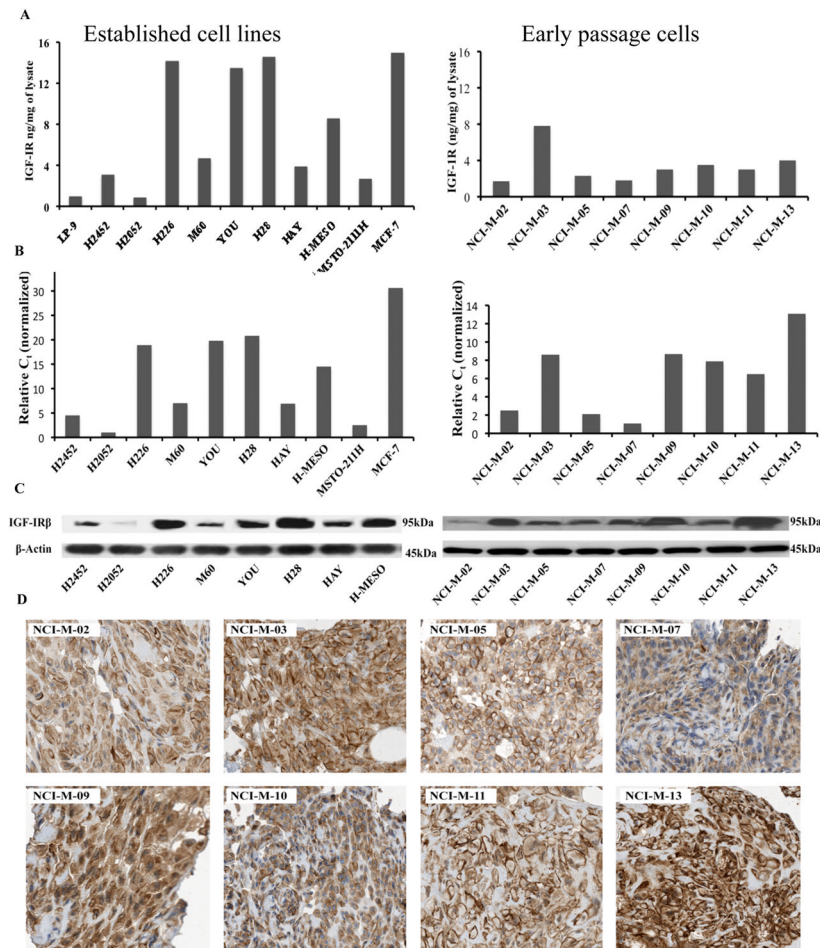


Figure 1. Determination of IGF-IR in mesothelioma cells. (A) IGF-IR level was quantitated using an ECL-based IGF-IR sandwich immunoassay. Results are expressed in terms of ng/mg of cell lysate. The breast cancer cell line MCF-7 and normal mesothelial cell line LP-9 were used as a positive and negative controls respectively. (B) IGF-IR mRNA in mesothelioma cell lines was determined with real-time qPCR analysis. mRNA levels were normalized to GAPDH mRNA levels. (C) IGF-IR protein was detected by immunoblotting with an anti-IGF-IR mAb. Experiments were done in triplicate and representative image has been shown for both IGF-IR and the loading control β -actin. (D) Tissue sections obtained from paraffin embedded cell blocks of early passage mesothelioma cells were evaluated for IGF-IR expression by IHC using an anti-IGF-IR polyclonal antibody. All of these early passage cells show both membranous and cytoplasmic staining for IGF-IR.

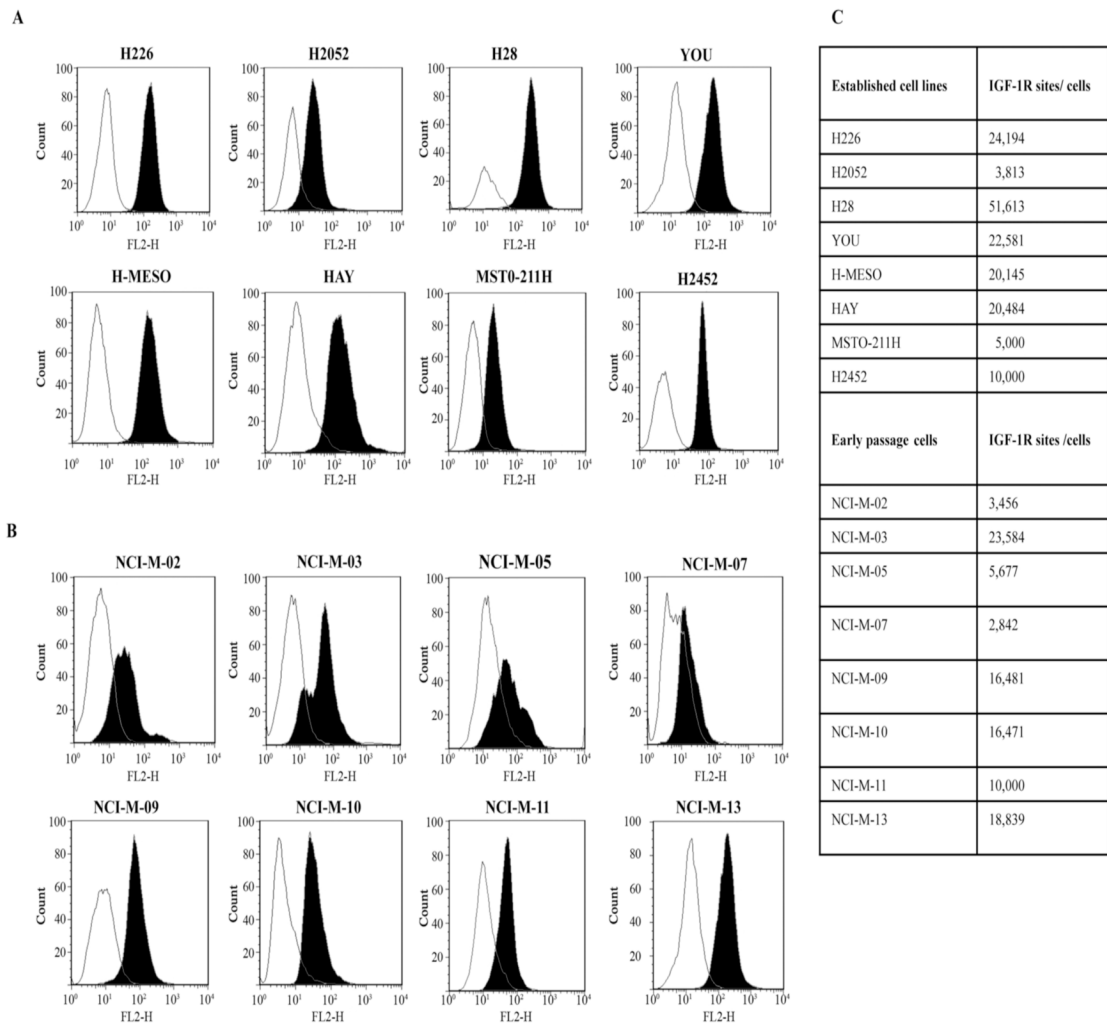


Figure 2. FACS analysis for cixutumumab binding in established (A) and in early passage (B) mesothelioma cells. Cells were incubated with cixutumumab or isotype control antibody at 4°C for 1 hr, followed by incubation with an anti-human antibody IgG–phycoerythrin conjugate. Results are shown in terms of histogram plot for each cell line depicting the binding of the cixutumumab (solid black) and the binding of isotype control antibody (white). (C) Table summarizing IGF-IR sites/cell in the mesothelioma cell lines that was determined using a cell surface IGF-IR quantitation assay.

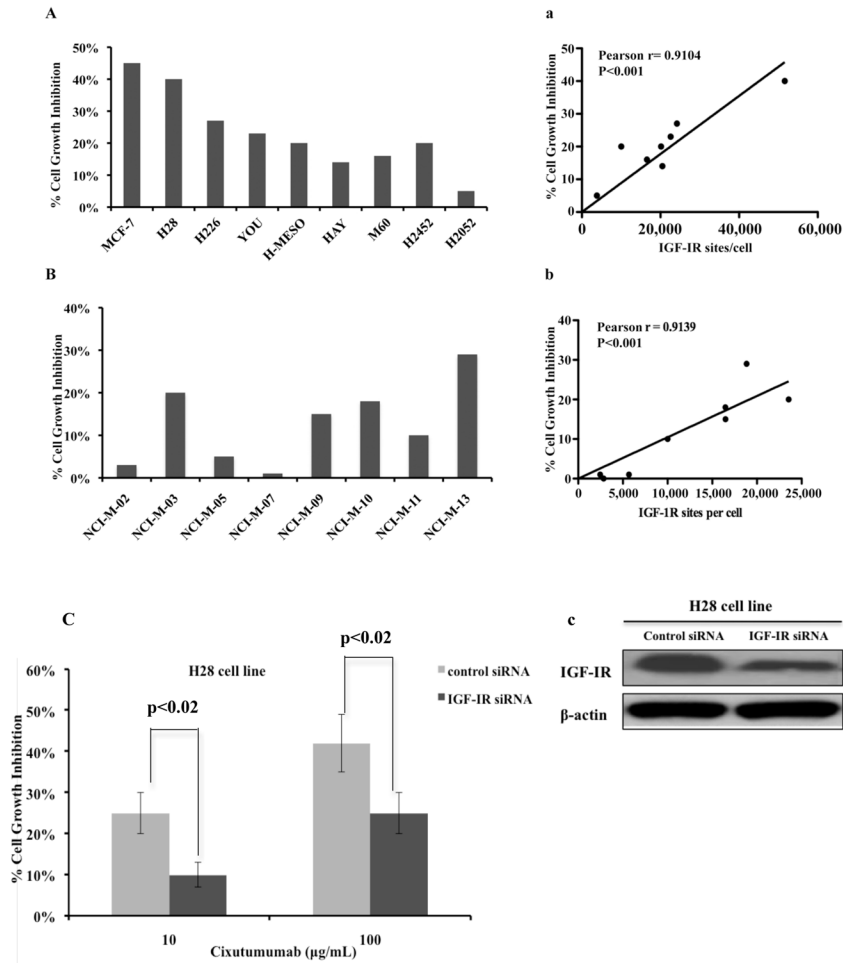


Figure 3.

Effect of cixutumumab on viability of established (A) and early passage (B) mesothelioma cells. The results are shown as % growth inhibition at 100 µg/mL of cixutumumab for each cell line. Pearson correlation analysis was performed using Graph pad to show the correlation between the activity of cixutumumab and surface IGF-IR sites/cell expressed by established (Aa) and early passage (Bb) mesothelioma cells. (C) H28 cells were treated with control si-RNA or IGF-IR siRNA for 48hr. Western blot analysis (Cc) was done to determine the expression level of IGF-IR after knockdown. Two days after transfection with either control si-RNA or IGF-IR si-RNA, H28 cells were treated with cixutumumab for 72 hr and cells viability was evaluated by ATP Lite assay. SD is shown for each treatment group. $p < 0.02$

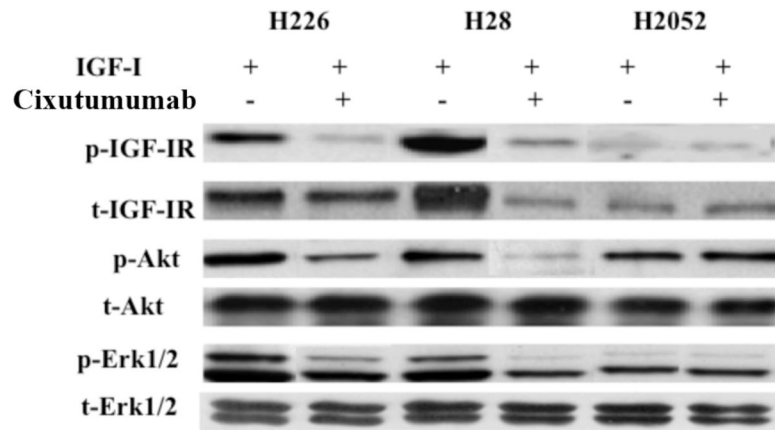


Figure 4. Effect of cixutumumab on IGF-IR downstream signaling pathway in H226, H28 and H2052 cell lines. Phosphorylation-dependent activation of downstream signaling molecules (p-IGF-IR, p-Akt and p-Erk) was analyzed by western blot with phosphorylation site-specific antibodies. Total protein expression of each molecule (t-IGF-IR, t-Akt and t-Erk) was analyzed.

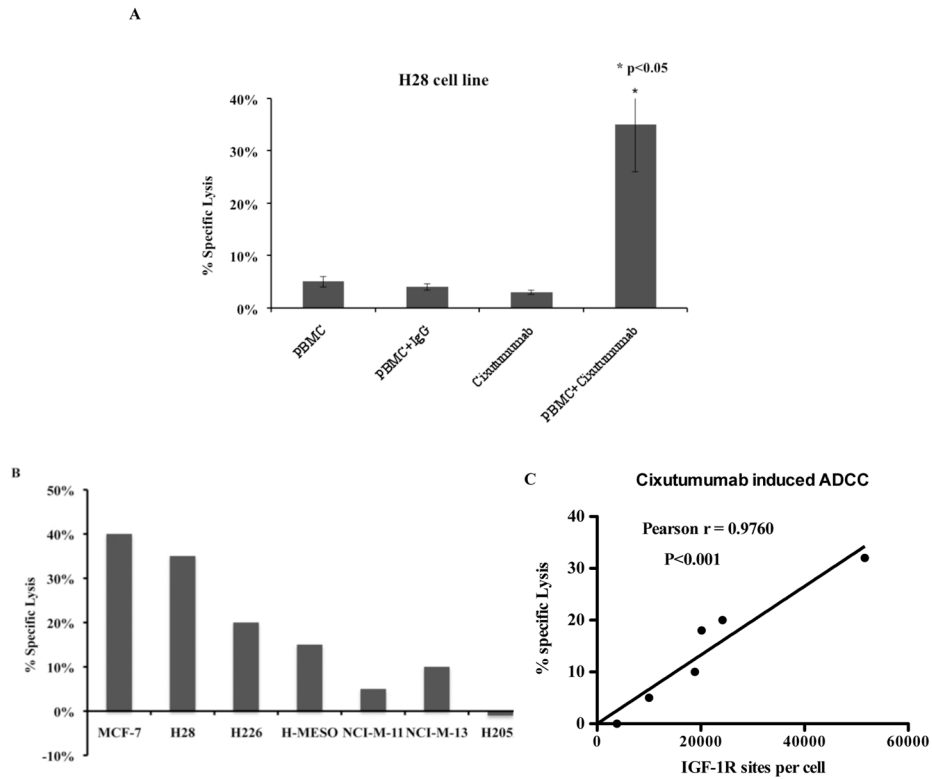


Figure 5.

Inductions of ADCC by cixutumumab in mesothelioma cell lines. Cells were incubated in the 96-well plate with 100 $\mu\text{g}/\text{mL}$ of cixutumumab or a control human IgG at 37°C for 1 hr followed by addition of the effector human peripheral mononuclear cells. The percentage of specific lysis was calculated using lactate dehydrogenase assay in (A) H28 cell line and (B) in panel of mesothelioma cell lines with varying degrees of IGF-IR expression. (C) Pearson correlation analysis was performed using Graph pad to show the correlation between ADCC induced by cixutumumab and IGF-IR sites/cell expressed by each cell line.

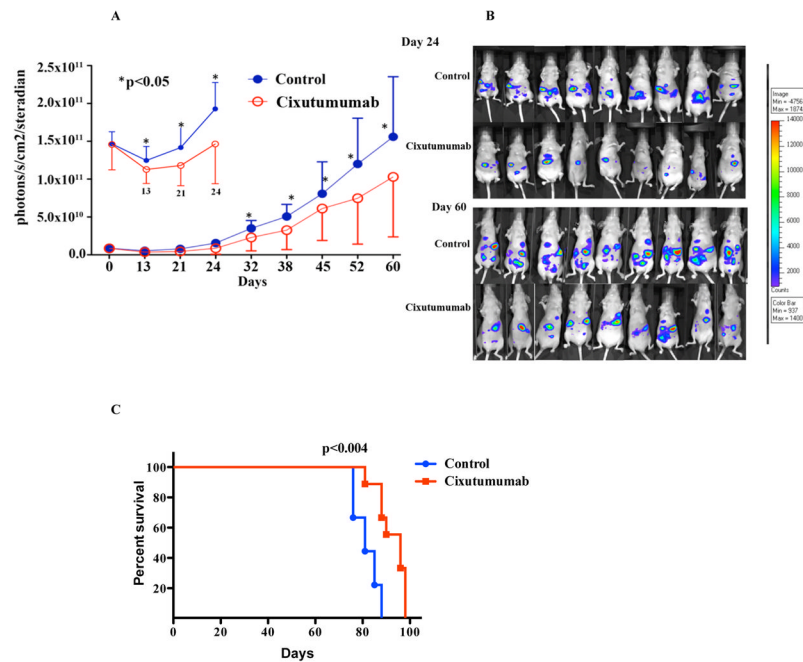


Figure 6.

Anti-tumor efficacy of cixutumumab in a mesothelioma xenograft model. Athymic nude mice were injected i.p. with 5×10^6 H226 mesothelioma cells and were randomized to receive either saline or cixutumumab 50 mg/kg i.p. (A) Graph shows significant decrease in the total flux counts in the cixutumumab treated group as compared to the saline treated group. Each data point is the median of 9 mice per treatment group. SD is shown for each point. * $P < 0.05$ (B) Whole-body non-invasive imaging of visible light emitted by luciferase expressing mesothelioma cells is shown for each mouse at days 24 and 60. (C) Kaplan-Meier curve showing the overall survival in cixutumumab treated group in comparison to saline treated control group.